

## Ultramicroanalysis of Y-Ba-Cu-O ceramics with the atom-probe microscope

Osamu Nishikawa and Masaharu Nagai

*Department of Materials Science and Engineering, The Graduate School at Nagatsuta,  
Tokyo Institute of Technology, 4259 Nagatsuta, Midori-ku, Yokohama 227, Japan*

(Received 21 September 1987)

We demonstrate that the atom-probe microscope has a unique capability for micro-mass-analyzing the Y-Ba-Cu-O superconducting ceramics. The analysis indicates that the ceramics contain extremely Cu-rich and Ba-rich regions. Even in a Y-Ba-Cu-O region with an appropriate composition the local composition varies noticeably over a range of 20–30 Å, which is a few times the perovskite lattice parameter.

The discovery of the 30-K transition-temperature  $\text{La}_{2-x}\text{Ba}_x\text{CuO}_{4-y}$  ceramic compound<sup>1</sup> led to the dramatic finding of the Y-Ba-Cu-O compound system, with a transition temperature  $T_c$  higher than 90 K.<sup>2</sup> The structure of these compounds is known to be an orthorhombic oxygen-deficient perovskite with a composition of  $\text{YBa}_2\text{Cu}_3\text{O}_{9-\delta}$ ,  $\delta=2.0$ .<sup>3</sup> It is natural that the composition of these sintered compounds is not uniform from the microscopic point of view.<sup>4</sup> Thus  $T_c$  and the critical current density  $I_c$  vary significantly from point to point depending on the local composition and structure. However, no detailed microscopic study has been conducted to clarify the variation of compositions and structures.

Recently it has been realized that the atom-probe microscope (APM)<sup>5</sup> would be a powerful instrument for the ultramicroanalysis of conducting ceramics.<sup>6</sup> The APM is a field-ion microscope (FIM)<sup>7</sup> with the atomically high resolution of  $\sim 2.5$  Å combined with a mass analyzer that can detect individual ions. When a positive high voltage, 5–20 kV, is applied to a specimen tip of the APM, the high field exerted above the tip apex induces the electrostatic evaporation of surface atoms. This phenomenon is called field evaporation<sup>7</sup> and the evaporation proceeds in an orderly atomic layer-by-layer fashion from the uppermost surface layer, breaking the weak bonds between the surface atoms and the substrate. Since some surface atoms evaporate as a cluster ion, reflecting the binding

state in the compound, the mass spectrum of the detected ions shed light on the binding states between atoms. The area analyzed by the APM is as small as a few angstroms to several tens of angstroms in diameter. Thus the number of surface atoms in the analyzed area is several to more than one hundred. Since the surface atoms evaporate atomic layer by layer, the detection sequence of ions shows the variation of the local composition with a lateral resolution of a few angstroms and a depth resolution of a single atomic layer.

Specimen ceramics were formed by mixing highly pure  $\text{Y}_2\text{O}_3$ ,  $\text{BaCO}_3$ , and  $\text{CuO}$  powders. Specimens were prepared by heating at 900 °C for 5 h in flowing oxygen and then pulverizing and reheating at 700 °C for 20 h. Although the resistance of all specimens went down to zero and the Meissner effect was exhibited at around 92 K,  $I_c$  varied from 20 to 3000 A/cm<sup>2</sup>. The local composition analyzed by the electron probe and x-ray microanalyzers with a spatial resolution of  $\sim 2$  μm scattered from Y:Ba:Cu varied from 1.0:0.77:0.93 to 1.0:2.56:4.50.

The specimen tip was prepared by cutting the ceramic disk to a rod 0.5 mm × 0.5 mm × 10 mm; one end of the rod was mechanically sharpened. The tip was introduced into the APM chamber of the vacuum of  $10^{-10}$  Torr and cooled down to 50 K. Although the tip was not sharp enough to observe FIM images, field evaporation of the surface layers proceeded smoothly when a tip voltage of 5

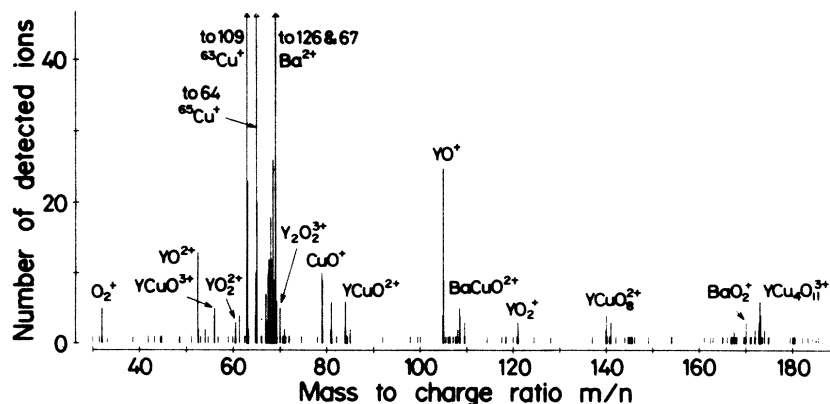


FIG. 1. Mass spectrum of ions detected from a Y-Ba-Cu-O compound. Fourteen ions with masses up to 388 are not shown.

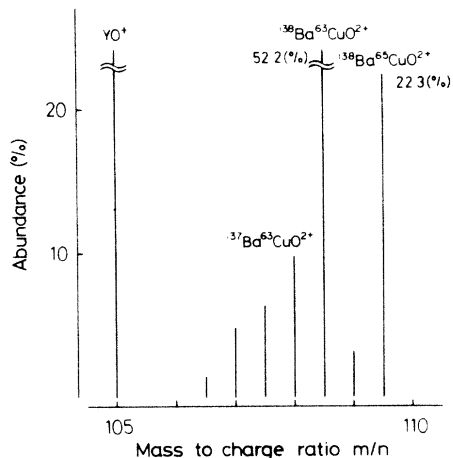


FIG. 2. Computer-simulated profile of mass peaks of  $YO^+$  and  $BaCuO^{2+}$ . Because the number of detected ions is small, the small peak with  $m/n = 109$  is not seen in Fig. 1.

to 13 kV and a nitrogen laser beam of 0.8 ns pulse width were applied to the tip.

Figure 1 is the mass spectrum of the detected ions. Mass peaks were identified by examining the heights of associated peaks of isotopes. For example, Y has no isotope while Cu has two mass peaks at  $m = 63$  and  $65$  and Ba has five isotopes. The computer-simulated profile of the mass peaks of  $YO^+$  and  $BaCuO^{2+}$ , Fig. 2, well agrees with the corresponding mass peaks of Fig. 1.

The interesting finding is that most Y atoms are detected as cluster ions such as of  $YO^+$ ,  $YCuO^+$ ,  $YO_2^+$ ,  $YCuO_8^{2+}$ , and  $YCu_4O_{11}^{3+}$ . On the other hand, Ba atoms were mostly detected as  $Ba^{2+}$  and a small number of  $BaCuO^{2+}$  and few  $BaO^+$ ,  $Ba_2O^{2+}$ , and  $BaO_2^+$  were found.

The variation of composition in a specimen can be manifested by counting the number of atoms in the detected ions. The cumulative number of counted atoms was plotted for each element in the detection sequency (Fig. 3). While the number of Y and Cu atoms increases linearly with the total number of atoms, the increase in Ba and O atoms is not monotonous but reciprocal to each other, that is, where the concentration of Ba is low, that of Cu is rather high. The average composition of the specimen shown in Figs. 1 and 3 is Y:Ba:Cu:O = 1.0:2.0:3.4:5.7. However, the local composition varies noticeably. For example, the

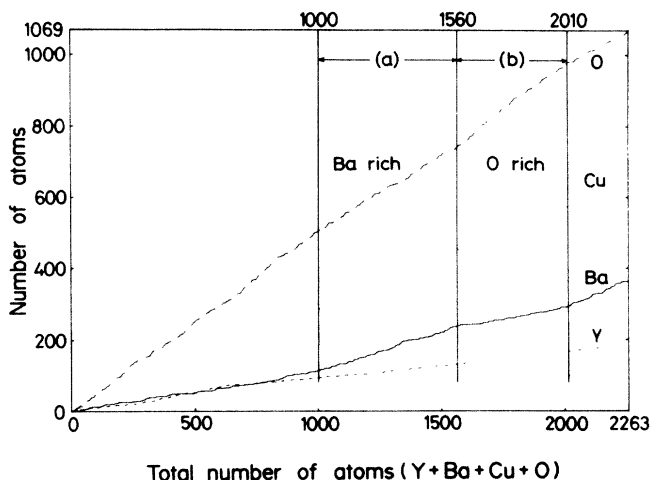


FIG. 3. Cumulative number of Y, Ba, Cu, and O atoms vs that of each element. Vertical lines indicate the boundaries of (a) Ba-rich and (b) O-rich sections.

compositions of two adjacent sections, (a) and (b) in Fig. 3, vary from the Ba-rich 1.0:2.7:3.6:5.0 to O-rich 1.0:1.6:3.4:6.9. The number of atoms detected from sections (a) and (b) is 560 and 450, respectively. Under the present experimental conditions, approximately 20 atoms are detected from an analyzed area of  $1 \text{ \AA}$  thickness. Thus the thickness of sections (a) and (b) is about 28 and 23  $\text{\AA}$ , respectively. This indicates that the local composition varies in the range of a few times the perovskite lattice parameter,  $11.6 \text{ \AA}$ .<sup>8</sup>

The composition of the specimens varied from extremely Cu rich to Ba rich. In the Cu-rich region neither Ba nor Y was found and most Cu atoms were detected as  $Cu^+$  and other ions were  $CuO^+$ ,  $Cu_2O^+$ ,  $Cu_3O^+$ ,  $Cu_3O_2^+$ , and  $CuO_2^+$  (see Fig. 4). An unexpected finding is the detection of  $Cu_2^+$  which is hardly detected in the analysis of metallic copper. The broad peaks to the right of  $^{65}Cu^+$  and  $^{65}CuO^+$  peaks could be the mass peaks of  $CuH_2^+$  and  $CuH_3^+$ .

The Ba-rich region is exhibited in the mass spectrum shown in Fig. 5. Ba atoms are detected as  $Ba^+$ ,  $BaO^+$ ,  $Ba_2O^+$ ,  $Ba_2O_2^+$ , and  $BaCuO^+$ , presenting a striking contrast to the spectrum of Fig. 1 where most Ba atoms are detected as  $Ba^{2+}$ .

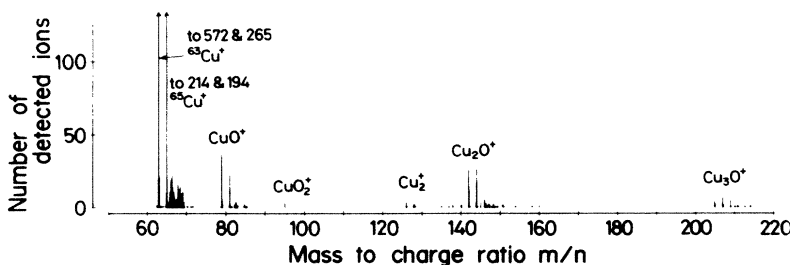


FIG. 4. Mass spectrum of Cu-rich region.

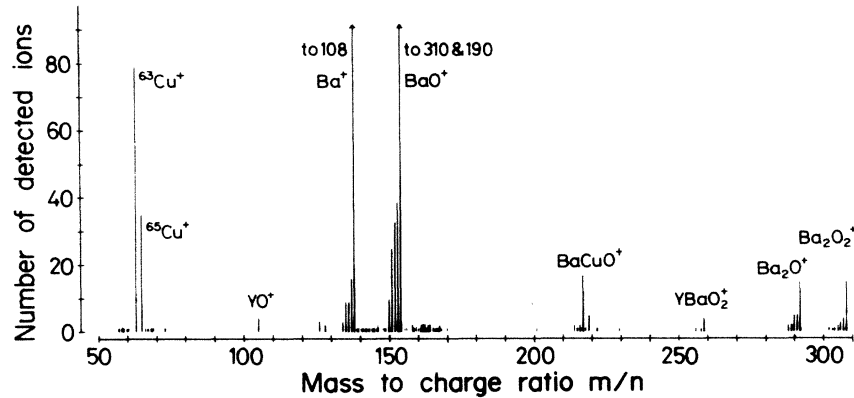


FIG. 5. Mass spectrum of Ba-rich region.

The difference in the ion species could be due to the variation of the binding states in the ceramics. Figure 6 shows the cumulative numbers of  $\text{Ba}^{2+}$ ,  $\text{Ba}^+$ , and  $\text{BaO}^+$  ions and Cu and Ba atoms detected from a Ba-rich region. While the number of Ba atoms increases linearly with the total number of atoms, the increase of Cu atoms is slightly steeper in the central section of the figure, indicated by the two vertical lines. The Ba ion species change abruptly from  $\text{Ba}^+$  and  $\text{BaO}^+$  to  $\text{Ba}^{2+}$  and vice versa at the boundaries of the Cu-rich section. Similar abrupt variation of ion species from  $\text{Ba}^+$ ,  $\text{TiO}_2^{3+}$ , and  $\text{TiO}_2^{2+}$  to  $\text{BaO}^+$  and  $\text{Ti}_2\text{O}_3^{3+}$  was observed at the polymorphic boundary in  $\text{Ba-TiO}_3$ .<sup>6</sup>

It is well known that these sintered compounds are porous.<sup>9</sup> Accordingly, when the encapsulated gas was released during the analysis, the pressure of the APM chamber rose momentarily from  $10^{-10}$  to  $10^{-9}$  Torr, in-

dicating that the volume of the cavity enclosing the gas is in the order of one cubic micron. The major components of the gas were found to be  $\text{H}_2$ ,  $\text{H}_2\text{O}$ ,  $\text{CO}$ , and  $\text{CO}_2$ . The frequency of gas burst reduced with lowering tip temperatures and the burst was hardly observed at 50 K.

The present study has successfully demonstrated that the APM has the unique capability of manifesting the variation of the composition in an extremely small region. It appears that the smaller the variation of the composition is, the larger the critical current density is. However, the clarification of the correlation between the current density, the variation of composition and the ion species requires a systematic and extensive long-range study because the volume of the analyzed region is extremely small compared to the grain size of the ceramics. Evaluation of the homogeneity of the ceramics formed by the coprecipitation method is under progress.

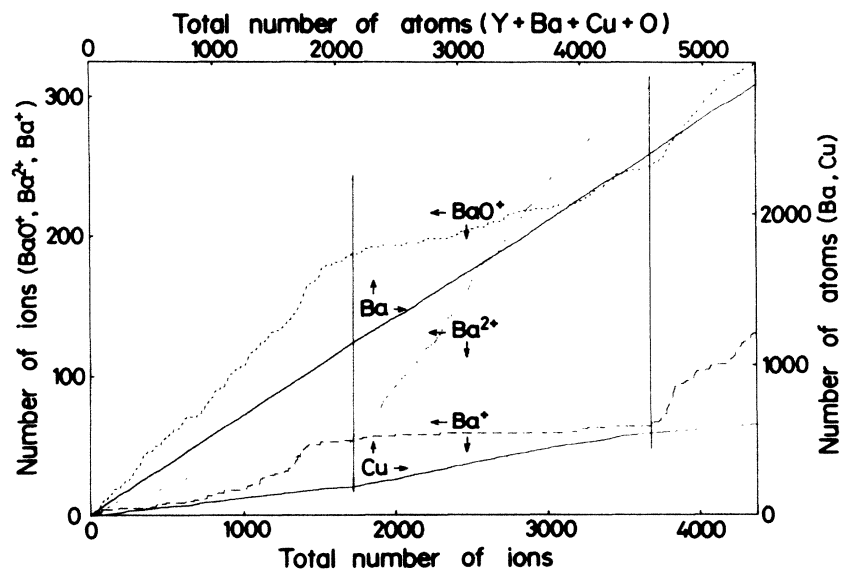


FIG. 6. Cumulative number of  $\text{Ba}^+$ ,  $\text{Ba}^{2+}$ , and  $\text{BaO}^+$  ions vs that of each ion species and that of Ba and Cu atoms vs that of each element. Vertical lines indicate the section where Cu concentration is high and most Ba atoms are detected as  $\text{Ba}^{2+}$ . Arrows point to the axes of corresponding ordinates and abscissas.

We take pleasure in acknowledging Dr. Y. Ishikawa of the Mechanical Engineering Research Laboratory of Hitachi, Ltd. for supplying the specimen ceramics. This work was supported by Grant-in-Aids for Scientific Research on Priority Areas and for Developmental Scientific Research by The Ministry of Education, Science, and Culture.

- 
- <sup>1</sup>G. Bednorz and K. A. Müller, *Z. Phys. B* **64**, 189 (1986).
- <sup>2</sup>C. W. Chu, P. H. Hor, R. L. Meng, L. Gao, Z. J. Huang, and Y. Q. Wang, *Phys. Rev. Lett.* **58**, 405 (1987); R. J. Cava, R. B. van Dover, B. Batlogg, and E. A. Rietman, *ibid.* **58**, 408 (1987); S. Uchida, H. Takagi, K. Kitazawa, and S. Tanaka, *Jpn. J. Appl. Phys.* **26**, L1 (1987).
- <sup>3</sup>T. Siegrist, S. Sunshine, D. W. Murphy, R. J. Cava, and S. M. Zahurak, *Phys. Rev. B* **35**, 7137 (1987); R. M. Hazen, L. W. Finger, R. J. Angel, C. T. Prewitt, N. L. Ross, H. K. Mao, C. G. Hadjidakos, P. H. Hor, R. L. Meng, and C. W. Chu, *ibid.* **35**, 7238 (1987); Y. LePage, W. R. McKinnon, J. M. Tarascon, L. H. Green, G. W. Hull, and D. M. Hwang, *ibid.* **35**, 7245 (1987).
- <sup>4</sup>S. X. Dou, A. J. Bourdillon, C. C. Sorrell, S. P. Ringer, K. E. Esterling, N. Savvides, J. B. Dunlop, and R. B. Roberts, *Appl. Phys. Lett.* **51**, 535 (1987).
- <sup>5</sup>E. W. Müller and S. V. Krishnaswamy, *Rev. Sci. Instrum.* **45**, 1053 (1974); O. Nishikawa, K. Kurihara, M. Nachi, M. Konishi, and M. Wada, *ibid.* **52**, 810 (1981).
- <sup>6</sup>O. Nishikawa, in *Proceedings of Semicon Osaka Technical Seminar 1987* (Semiconductor Equipment and Materials Institute, 1987), p. 289.
- <sup>7</sup>E. W. Müller and T. T. Tsong, *Field Ion Microscopy, Principles and Applications* (Elsevier, New York, 1968).
- <sup>8</sup>P. M. Grant, R. B. Beyers, E. M. Engler, G. Lim, S. S. P. Parkin, M. L. Ramirez, V. Y. Lee, A. Nazzal, J. E. Vazquez, and R. J. Savoy, *Phys. Rev. B* **35**, 7242 (1987).
- <sup>9</sup>D. S. Ginley, E. L. Venturini, J. F. Kwak, R. J. Baughman, B. Morosin, and J. E. Schirber, *Phys. Rev. B* **36**, 829 (1987).